



**HAL**  
open science

## Comparison of EMG-to-torque models using an upper-limb exoskeleton

Lucas Quesada, Dorian Verdel, Olivier Bruneau, Bastien Berret, Michel-Ange Amorim, Nicolas Vignais

► **To cite this version:**

Lucas Quesada, Dorian Verdel, Olivier Bruneau, Bastien Berret, Michel-Ange Amorim, et al.. Comparison of EMG-to-torque models using an upper-limb exoskeleton. 48e Congrès de la Société de Biomécanique, Société de Biomécanique, Oct 2023, Grenoble, France. hal-04204184

**HAL Id: hal-04204184**

**<https://universite-paris-saclay.hal.science/hal-04204184>**

Submitted on 11 Sep 2023

**HAL** is a multi-disciplinary open access archive for the deposit and dissemination of scientific research documents, whether they are published or not. The documents may come from teaching and research institutions in France or abroad, or from public or private research centers.

L'archive ouverte pluridisciplinaire **HAL**, est destinée au dépôt et à la diffusion de documents scientifiques de niveau recherche, publiés ou non, émanant des établissements d'enseignement et de recherche français ou étrangers, des laboratoires publics ou privés.



Distributed under a Creative Commons Attribution 4.0 International License

# Comparison of EMG-to-torque models using an upper-limb exoskeleton

L. Quesada<sup>a,b,c\*</sup>, D. Verdel<sup>a,b,c</sup>, O. Bruneau<sup>c</sup>,  
B. Berret<sup>a,b</sup>, M-A. Amorim<sup>a,b</sup>, N. Vignais<sup>a,b</sup>

<sup>a</sup>CIAMS, Université Paris-Saclay, Orsay, France;

<sup>b</sup>CIAMS, Université d'Orléans, Orléans, France ;

<sup>c</sup>LURPA, ENS Paris-Saclay, Gif-sur-Yvette, France

## 1. Introduction

Work-related musculoskeletal disorders (MSDs) pose significant challenges to society. To reduce the incidence of MSDs, current solutions rely on developing ergonomic workplaces or adapting work tasks. A promising alternative aims to compensate for MSD-causing efforts by using active exoskeletons. However, an accurate estimation of the operator's intention is crucial for providing timely and appropriate assistance (Bi et al. 2019). One potential method is to utilize electromyographic (EMG) signals for estimating joint torques and determining suitable assistance (Treussart et al. 2020). The present study aims to compare the ability of different EMG-to-torque models to estimate elbow torque.

## 2. Methods

### 2.1 Participants

Ten healthy participants (3 F, 29.4±6.6y, 72.6±11.0 kg, 175.7±4.4 cm) participated in this study and signed a written informed consent. The protocol was approved by an ethics committee (CER-PS-2021-048/A1).

### 2.2 Material

EMG signals were recorded from seven muscle heads at a frequency of 2 kHz (MiniWave, Cometa, Italy). Electrodes were placed following SENIAM recommendations on the lateral, medial, and long triceps, the long and short biceps, the brachialis, and the brachioradialis. The elbow axis of the ABLE upper limb exoskeleton (Garrec et al. 2008) was used in resistive mode, applying a viscous force field during flexion and extension movements to impose a torque perturbation on the elbow (based on a normalized subjective effort using a Borg scale). The participant was attached to the exoskeleton at wrist level through an adapted orthosis under which a 6-axis force/torque (FT) sensor allowed the measurement of the perturbation applied by the exoskeleton on the forearm. Kinematic data were recorded using an optoelectronic system (Qualisys, Sweden). Target trajectory and elbow angle visual feedback were projected onto a screen in front of the participant.

### 2.3 Procedure

EMG sensors were placed on the participant's muscles, and maximal voluntary contraction (MVC) was

performed after verifying sensor location. Reflective markers were placed on anatomical landmarks for limb measurement and kinematics. After being attached in the exoskeleton with their arm immobilized, the participant was asked to track a 30s randomized trajectory projected on the screen, implying elbow flexion and extension. Each participant performed ten trials.

### 2.4 Data processing

EMG signals were processed using a 20-450 Hz bandpass filter, a rectification, and a 3 Hz low pass filter (Lotti et al. 2022). They were then normalized with MVC. Interaction torque ( $\tau_i$ ) was computed using inverse dynamics from the exoskeleton's FT sensor. Dynamic torques of the forearm ( $\tau_{dyn}$ , gravitational and inertial) were estimated using inertial data from anthropometric tables. The net human torque  $\tau_h$  is then  $\tau_h = \tau_{dyn} + \tau_i$  and is the reference value.

### 2.5 Model validation

A cross-validation method was used to evaluate EMG-to-torque models: they were each first calibrated on one trial and then used to estimate torques (*i.e.*  $\hat{\tau}_h$ ) on the other nine trials. A normalized root mean square error (NRMSE) was computed for each of the nine estimates, comparing  $\tau_h$  and  $\hat{\tau}_h$ . This process was repeated for each of the ten trials in turn, with one serving as calibration and the others as validation. The mean NRMSE for each model was then computed.

### 2.6 Statistical analysis

Normality was first assessed (Shapiro-Wilk), and a repeated measures analysis of variance (RmANOVA) was performed to test model differences. A post hoc test was then performed using a Bonferroni correction.

## 3. EMG-to-torque Models

In the following section, EMG-to-torques models are described using  $k$  muscles and  $j$  degrees of freedom. Data matrices contain  $n$  samples. Models were chosen based on common occurrences in literature.

### 3.1 Multivariate linear regression

The multivariate linear regression (MVLRL) model was used as a baseline for comparison (Camardella et al. 2021). It is a linear relationship between muscle excitations and torques:

$$\boldsymbol{\tau}(t) = \mathbf{C} \cdot \mathbf{m}(t)$$

where  $\mathbf{C} \in \mathbb{R}^{j \times k}$  is the muscle mapping matrix,  $\boldsymbol{\tau} \in \mathbb{R}^j$  the torque vector and  $\mathbf{m} \in \mathbb{R}_+^k$  the muscle excitation vector. The muscle mapping matrix is computed using multivariate regression on calibration data matrices  $\mathbf{T}_c \in \mathbb{R}^{j \times n}$  and  $\mathbf{M}_c \in \mathbb{R}_+^{k \times n}$  containing respectively torque and muscle excitation sample vectors.

### 3.2 Synergies

Synergy-based models (SYN) are described as a coherent activation in space and time of groups of muscles (Delis et al. 2014). Spatial synergies can be extracted from muscle excitations using non-negative matrix factorization:

$$\mathbf{M}_c = \mathbf{W} \cdot \mathbf{H}_c + \boldsymbol{\varepsilon}$$

with  $\mathbf{H}_c \in \mathbb{R}_+^{s \times n}$  the synergy activation matrix corresponding to the calibration data, and  $\mathbf{W} \in \mathbb{R}_+^{k \times s}$  the synergy matrix, mapping a synergy activation to a group of muscles. In this formulation,  $s$  is the number of extracted synergies and  $\boldsymbol{\varepsilon} \in \mathbb{R}^{k \times n}$  is the matrix of factorization residuals. After factorization, the torque is computed in a similar way to the MVLR model:

$$\boldsymbol{\tau}(t) = \mathbf{C}_s \cdot \mathbf{W}^+ \cdot \mathbf{m}(t)$$

with  $\mathbf{C}_s \in \mathbb{R}^{j \times s}$  the synergy mapping matrix computed using multivariate regression on calibration data matrices  $\mathbf{T}_c$  and  $\mathbf{H}_c$ , and  $\cdot^+$  is the pseudo inverse. This model was tested with two to seven synergies.

### 3.3 Neuromusculoskeletal

Neuromusculoskeletal (NMS) models combine musculoskeletal and Hill-type neuromuscular models. A generic OpenSim model (Holzbaur et al. 2005) is first scaled using kinematic data. Muscle activation  $a$  is then derived from excitations via a non-linear shape factor and each muscle force is computed from a Hill-type model (Buchanan et al. 2004):

$$F_m = F_0 \left( a f^L(\tilde{l}) f^V(\tilde{v}) + f^{PE}(\tilde{l}) \right) \cos(\alpha)$$

where  $F_0$  is the maximum isometric force,  $f^L$  and  $f^V$  are respectively the force-length and force-velocity relationships,  $\tilde{l}$  and  $\tilde{v}$  are the normalized length and velocity of the muscle fiber, and  $\alpha$  is the muscle pennation angle. The passive elastic behavior of the muscle fiber is represented by  $f^{PE}$ . Finally, the joint torque  $\boldsymbol{\tau}$  was obtained by summing muscle forces weighted by the muscle's moment arm projected on the joint axis. A genetic algorithm was used to optimize five parameters per muscle from calibration data: max isometric force, tendon slack length, optimal pennation angle, optimal fiber length, and shape factor.

## 3. Results and discussion

Calibration took an average of ten minutes for NMS and less than one second for MVLR and SYN. Estimation time was several milliseconds for NMS and less than one millisecond for MVLR and SYN. The NMS and MVLR models produced a mean NMRSE of  $7.35\% \pm 1.2$  and  $8.73\% \pm 1.4$ , respectively. SYN models ranged from  $9.68\% \pm 2.5$  to  $8.69\% \pm 1.4$ . (Figure 1). Overall, the NMS model allowed for significantly ( $p < 0.01$ ) better torque reconstruction than any other model with a large effect size (Cohen's

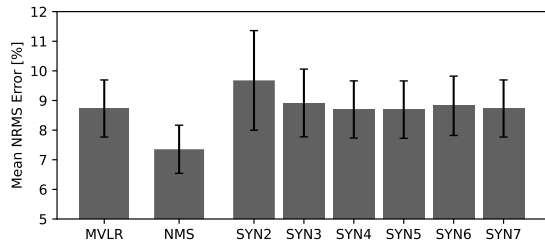


Figure 1 Mean normalized root mean square error of validation trials for each model. Error bars represent the 95% confidence interval.

$d > 0.8$ ). MVLR and SYN models did not show significant differences. While the NMS model is more accurate than the other models, other criteria such as calibration and estimation times should be considered for application purposes (Bi et al. 2019). In this context, the performance of the NMS model may not be worth its computational cost against MVLR. To ensure applicability in industrial settings, it is crucial to expand these findings to multiple joints, considering the potential influence of biarticular muscles on the results. Additionally, it is important to investigate the impact of EMG signal degradation caused by factors such as sweat, fatigue, and electrode displacement.

## 4. Conclusions

In the present preliminary study, we compared three EMG-to-torque models using a specific in situ procedure. We showed that the NMS model was significantly more accurate than MVLR and SYN models. Future work will extend this study to include more degrees of freedom and criteria to guide the selection of models for real-time applications.

## References

- Bi L, Feleke A, Guan C. 2019. A review on EMG-based motor intention prediction of continuous human upper limb motion for human-robot collaboration. *Biomed. Signal Process. Control*.
- Buchanan TS, Lloyd DG, Manal K, Besier TF. 2004. Neuromusculoskeletal Modeling: Estimation of Muscle Forces and Joint Moments and Movements from Measurements of Neural Command. *J. of App. Biomech*.
- Camardella C, Barsotti M, Buongiorno D, Frisoli A, Bevilacqua V. 2021. Towards online myoelectric control based on muscle synergies-to-force mapping for robotic applications. *Neurocomp.*,
- Delis I, Panzeri S, Pozzo T, Berret B. 2014. A unifying model of concurrent spatial and temporal modularity in muscle activity. *J. Neurophysiol*.
- Garrec P, Friconeau J P, Measson Y, Perrot Y. 2008. ABLE, an innovative transparent exoskeleton for the upper-limb. *IEEE/RSJ IROS*.
- Holzbaur K, Murray W, Delp S. 2005. A Model of the Upper Extremity for Simulating Musculoskeletal Surgery and Analyzing Neuromuscular Control. *Ann. Biomed. Eng.* ,
- Lotti N, Xiloyannis M, Missiroli F, Bokranz C, Chiaradia D, Frisoli A, Riener R, Masia L. 2022. Myoelectric or Force Control? A Comparative Study on a Soft Arm Exosuit. *IEEE Trans. Rob.*
- Treussart B, Geffard F, Vignais N, Marin F. 2020. Controlling an upper-limb exoskeleton by EMG signal while carrying unknown load. *IEEE ICRA*.

**Keywords:** electromyography; intention detection; torque estimation; exoskeleton

**\*Corresponding author. Email:**

**[lucas.quesada@universite-paris-saclay.fr](mailto:lucas.quesada@universite-paris-saclay.fr)**